Mon. Not. R. Astron. Soc. **000**, 000–000 (0000) Printed 16 August 2007 (MN LATEX style file v1.4)

The SCUBA Bright Quasar Survey II: unveiling the quasar epoch at submillimetre wavelengths

Robert S. Priddey[1], Kate G. Isaak[2], Richard G. McMahon[3] & Alain Omont[4]
[1] *Astrophysics Group, Imperial College, Blackett Laboratory, Prince Consort Road, London SW7 2BZ*
[2] *Cavendish Astrophysics, University of Cambridge, Cambridge CB3 0HE*
[3] *Institute of Astronomy, Madingley Road, Cambridge CB3 0HA, UK*
[4] *Institut d'Astrophysique de Paris, CNRS, 98bis Bd. Arago, Paris, France*
email: r.priddey@ic.ac.uk, isaak@mrao.cam.ac.uk, rgm@ast.cam.ac.uk

Accepted for publication in MNRAS, 14th November 2002

ABSTRACT

We present results of the first systematic search for submillimetre (submm) continuum emission from $z \sim 2$, radio-quiet, optically-luminous ($M_B < -27.5$) quasars, using the SCUBA array camera on the JCMT. We have observed a homogeneous sample of 57 quasars in the redshift range $1.5 < z < 3.0$— the epoch during which the comoving density of luminous AGN peaks— to make a systematic comparison with an equivalent sample at high redshift ($z > 4$; Isaak et al., 2002: Paper I). The target sensitivity of the survey, $3\sigma = 10$mJy at 850μm, was chosen to enable efficient identification of bright submm sources, suitable for detailed follow-up. 9 targets are detected with 3σ significance or greater, with fluxes in the range 7–17mJy. Although the detection rate above 10mJy is lower than that of the $z > 4$ survey, the weighted mean flux of the undetected sources, 1.9±0.4mJy, is similar to that at $z > 4$ (2.0±0.6mJy). The statistical significance of trends is analysed, and it is found that: (i) within the limited optical luminosity range studied, there is no strong evidence for a correlation between submm and optical luminosity; (ii) there is a suggestion of a variation of submm detectability with redshift, but that this is consistent with the K-correction of a characteristic far-infrared spectrum.

Key words: dust, extinction – quasars: general – galaxies: starburst – cosmology: observations – submillimetre

1 INTRODUCTION

By virtue of their high, sustained luminosity across the spectrum, quasars are ideal targets for studies of the evolution of structure throughout the history of the cosmos. Whilst a rare phenomenon in our local volume of space, the comoving density of luminous AGN rises sharply as one goes back in time, to a peak (Schmidt, Schneider & Gunn., 1995; Fan et al. 2001) or a plateau (Miyaji, Hasinger & Schmidt, 2000) around z=2, an epoch dependence echoing the star formation history of galaxies (e.g. Madau et al. 1996; Steidel et al. 1999). It is widely believed that most massive galaxies undergo a short-lived AGN phase, as they build up the supermassive black holes observed in local galactic cores (Magorrian et al., 1998). Thus in observing a quasar, one catches its host galaxy at a significant period in its evolution.

At far-infrared (FIR) to millimetre (mm) wavelengths, AGN have long been recognised as amongst the most prominent high-redshift sources (e.g. the compilations in McMahon et al., 1999 (M99); Rowan-Robinson, 2000). While there is strong evidence that emission from this region of the spectrum is thermal reradiation from warm dust (e.g. Hughes et al., 1993), it is not always clear that the AGN itself is the sole contributor to dust heating, and it is plausible that a fraction of the submm luminosity could derive from stars in the surrounding galaxy. There would thus be a direct overlap between dusty quasars and SCUBA survey sources, which, it is argued, are the star-forming progenitors of massive spheroids. Hence, targetted submm and mm surveys of high-redshift AGN are valuable in elucidating the nature of cosmological submm sources, and the relation between the evolution of the host galaxy and its central black hole.

M99 observed a small sample of $z > 4$, radio-quiet quasars with the JCMT's SCUBA submm camera to high sensitivity ($\sigma_{850\mu m} \approx 1.5$mJy), to determine the submm properties of the "typical" high-redshift AGN. A complementary, broad-but-shallow ($\sigma_{850\mu m} \approx 3$mJy) strategy was adopted by Isaak et al. (2002: I02)— the SCUBA Bright Quasar Survey (SBQS) (Paper I)— with the principal aim of defining a statistically-significant sample of submm sources bright enough to permit a range of follow-up study. Roughly

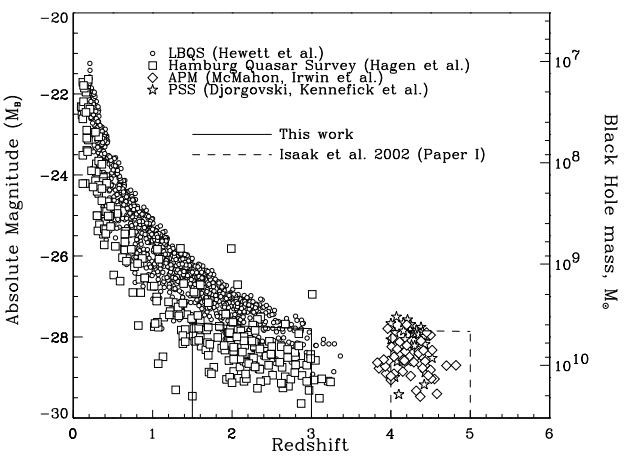

Figure 1. Hubble diagram for quasar surveys used in the Paper I (Isaak et al. 2002, $z > 4$ selection) and the present work ($z \approx 2$ selection). Note that in each case, the optical luminosity was designed to be $M_B < -27.5$ *in the EdS cosmology* for consistency with previous work. This is converted to the Λ cosmology employed in this paper, but it is clear that the difference between the samples is small. The black hole mass (right-hand axis) is calculated from M_B assuming accretion at the Eddington rate.

a quarter of the targets were brighter than the $3\sigma \sim 10$mJy limit, suggesting that a substantial fraction of high-redshift quasars have far-infrared luminosities comparable to their blue luminosities. A natural question is whether this ubiquitous submm activity discovered at $z > 4$ is typical of high-redshift AGN in general: is the optically-luminous quasar phase always accompanied by a dust-rich submillimetre source, or does this only occur at the highest redshifts? In the current paper we present the results of a comparative survey designed to address this question, targetting the "AGN epoch" at $z \sim 2$, the era at which the space density of quasars reaches its maximum, and by which most (> 80 percent) of the matter that will ever be accreted onto supermassive black holes has already served as fuel for AGN. A presentation of these results, along with brief analysis, is the purpose of the current paper: a more detailed and wide-ranging study, in the context of all the recent mm and submm quasar surveys in this series (M99; I02; Omont et al., 2001; Omont et al., 2002), will be given in a forthcoming work (Priddey et al., in prep.).

We assume the currently-favoured Λ-dominated cosmology Ω_M=0.3, Ω_Λ=0.7, H_0=65 km s^{-1} Mpc^{-1} (Λ). For continuity with previous work, we will give alternatives in an Einstein–de Sitter cosmology, Ω_M=1, Ω_Λ=0, with H_0=50 km s^{-1} Mpc^{-1} (EdS).

2 SAMPLE SELECTION AND OBSERVATIONS

Our aim was to find a sample of bright, medium-redshift quasars well-matched to the $z > 4$ sample observed by Isaak et al. (2002) (Figure 1). To avoid too heterogeneous a sample, we restricted the input catalogues to a few large, homogeneous surveys. The final target list comprises quasars preselected from the Large Bright Quasar Survey (LBQS: Hewett, Foltz & Chaffee, 1995) and the Hamburg Quasar Survey (HS: Engels et al. 1998; Hagen et al. 1999). The first selection criterion is based on optical luminosity represented by absolute B-band magnitude (M_B). At $z = 2$, the J photometric band samples very close to rest-frame B, and H starts to do so towards higher redshifts. Using a combination of these bands therefore gives an absorption-free assessment of the rest-frame optical magnitude, minimizing the error due extrapolation of the continuum. This overcomes many of the problems encountered when deriving M_B for $z > 4$ quasars— e.g. contamination of the R band by strong emission and absorption features (as detailed in Paper I). Similarly, at $z \approx 2$, observed-frame B becomes compromised by the strong CIV and Ly-α emission lines.

Hence, to obtain a sample of luminous $z \approx 2$ quasars all with J and H magnitudes, we cross-correlated catalogues of bright, medium-redshift quasars with the 2MASS near-infrared catalogue through the web-based interface at IPAC (http://www.ipac.caltech.edu). Counting sources out to a radius of 60 arcsec enabled us to determine a maximum association radius of 5 arcsec, within which the probability of a chance association is <0.5 percent. Absolute B-band magnitudes were calculated from apparent J and H magnitudes thereby obtained (all our targets were detected in both bands) weighted according to the proximity of the band to B in the redshifted spectrum. They have been corrected for Galactic extinction, though in most cases this is negligible (< 0.05mag). We have assumed an optical spectral index $\alpha_{\rm opt} = -0.5$ (where $f_\nu \propto \nu^\alpha$), though, as noted, the extrapolation error is small. Photometric errors in J and H are typically 0.1–0.2mag.

In order to match optical luminosity with the $z > 4$ sample, objects with $M_B^{\rm EdS} < -27.5$ were initially selected— i.e. adopting the same cosmology as per the selection of the $z > 4$ sample*. A wide redshift range $1.50 < z < 3.00$ was chosen to maximize the potential number of targets (Figure 1). To derive an observing sequence, the final selection was prioritized according to optical luminosity, the most luminous given preference.

The nominal completeness limit for 2MASS is 15.8 and 15.1 in J and H respectively. However, at the high Galactic latitudes inhabited by these quasars, accurate detections up to one magnitude better than this can be achieved (Cutri et al., 2000). From this and our extensive quasar catalogue cross-correlations with 2MASS, we estimate that at $z = 3$, the 2MASS limit corresponds to $M_B^{\rm EdS} \approx -27.6$, thus for the greater extent of our redshift range we are not in danger of overlooking bright potential targets that failed to be detected by 2MASS.

The target list was correlated with the NRAO VLA Sky Survey (NVSS) to identify radio-loud sources, which were excised from the list. As discussed in M99 and I02, "radio loud" in this context primarily refers to the extent of contamination of the thermal submm continuum by the extrapolated radio synchrotron. Assuming a spectral index

* Note that this selection was made in the EdS cosmology; as shown in Figure 1 and Table 1, converting to the Λ cosmology introduces an average shift of -0.2mag. Most importantly, the overall difference between the $z = 2$ and $z > 4$ samples is small.

$\alpha = -0.5$, a source with $S_{1.4\mathrm{GHz}} < 1.5$mJy (below the NVSS limit) will have $S_{850\mu\mathrm{m}} < 0.1$mJy.

The JCMT observing strategy for this project was the same as for the comparable $z > 4$ program described in detail in I02. To reiterate: the required RMS ($1\sigma = 3$mJy) can be reached in a short amount of observing in relatively poor (zenith transmission 65%) weather, so the JCMT fallback queue was utilized. SCUBA was employed in photometry mode, that is, the source is placed on the central bolometer, while the rest of the array samples the sky. Flux calibration was determined from the planets Mars and Uranus, or from secondary continuum standards (CRL618, OH231.8, IRC10216). The APM catalogue (online interface http://www.ast.cam.ac.uk/∼apmcat) was used to verify coordinates, which are given in Table 1.

3 RESULTS AND COMMENTARY

A total of 57 $z \sim 2$ quasars have been observed with SCUBA in the current survey, 9 of which are detected with $>3\sigma$ significance at 850μm. The median RMS flux is $\sigma_{850} = 2.8$mJy, with a narrow (0.4mJy) interquartile range. Four of the sources have $3\sigma > 10$mJy: in the following analysis, we exclude these from our complete statistical sample, which thus consists of 53 sources.

One detection, the $z = 2.6$ quasar LBQS B0018−0220, is significantly brighter than the nominal 10mJy limit: with $S_{850} = 17 \pm 3$mJy, this is an exceptionally bright source, comparable to some of the brightest high-redshift submm sources known. To recover most of the other detections, one must go down to ≈ 8mJy. In contrast, seven of the eight detections from the $z > 4$ SCUBA Bright survey (I02) lie above 10mJy. In Figure 2, 850μm fluxes of the $z \sim 2$ sources reported in this paper are plotted along with the $z > 4$ sample described in I02. The curves represent the flux one would observe from an object of fixed luminosity as a function of redshift, assuming it has the mean far-infrared SED determined from $z > 4$ quasars by Priddey & McMahon (2001: PM01), characterized by an isothermal temperature and emissivity index $T = 40$K and $\beta = 2$, respectively. The large K-correction towards high redshift is one possible reason why the $z > 4$ sources appear systematically brighter, however it is not obvious that the same SED is valid for all objects at all redshifts. (Indeed, one of the motivations for *this* project was to yield a sample bright enough to be studied at a number of submm wavelengths, so that the typical FIR SED of a $z = 2$ quasar could be determined.)

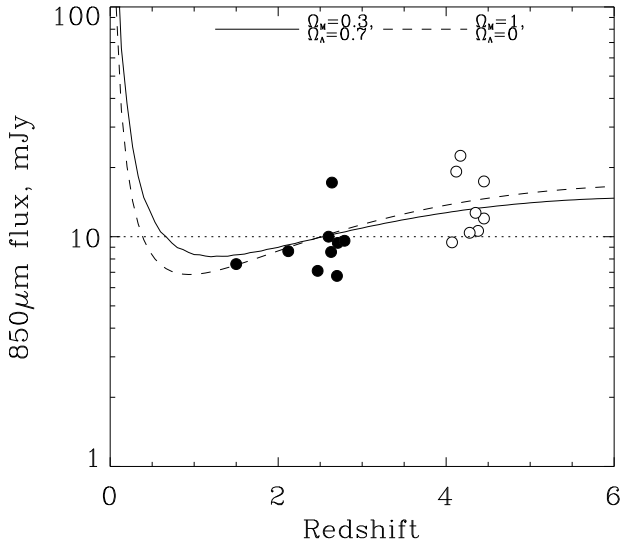

Figure 2. Flux at 850μm against redshift, plotted for SBQS detections from Paper I (I02, open symbols) and the current work (filled symbols). The dotted line represents the nominal 3σ=10mJy limit for this work, the approximate threshold for viable follow-up such as CO line detection. The two curves are, for two different cosmologies, the flux one would detect from a source of fixed luminosity having the mean isothermal SED of PM01 ($T = 40$K, $\beta = 2$). They are arbitrarily normalized, and are plotted only to illustrate the necessary K-correction between the redshift ranges of the two surveys.

4 STATISTICAL ANALYSIS

4.1 Submillimetre versus optical

Figure 3 shows 850μm fluxes plotted against absolute magnitudes for the $z \approx 2$ sample. (NB: we do not correct the optical for intrinsic absorption.) Any correlation between submm and optical is even less evident than in the case of the $z > 4$ sources of I02. This can be demonstrated formally using statistical tests. If there were a correlation between detectability and absolute magnitude, we might expect the detected sources to be distributed with respect to M_B in a different way than the whole sample. Applying the Kolmogorov–Smirnov (K–S) test informs us that the null hypothesis that the distributions are the same Note that, unlike the $z > 4$ objects, this material is less prone to systematic error in the determination of M_B: the magnitudes were calculated homogeneously, and the need for continuum extrapolation was minimized. Yet, the scatter remains, which suggests that it derives from an underlying variance in the submm–optical relation.

As discussed in I02, one might naively expect a submm–optical correlation, whether the dust-heating source is stars (because spheroid mass scales with black hole mass) or the AGN (because both L_{FIR} and L_B scale with bolometric luminosity). There is much scope for complexity which would smear out any correlation, for example the relative timing between AGN fuelling and starburst, or, in an AGN-powered scenario, the effects of varying the dust-torus geometry. As a *caveat*, note that the nominal detection threshold, 10mJy, corresponds, at $z = 2$, to $L_{\mathrm{FIR}} \approx 2 \times 10^{13}\,\mathrm{L}_\odot \approx \nu L_B$ for the value of the magnitude cut, $M_B = -27.5$. We are therefore probably sampling only the bright tail of the FIR luminosity distribution, and we are biased towards sources lying just above this $L_{\mathrm{FIR}} \approx \nu L_B$ threshold. Thus for the detected sources, any such relation should be derived with caution.

4.2 Optical colour

As described in Section 2, 2MASS J and H magnitudes were obtained primarily to provide a homogeneous optical luminosity scale, directly sampling rest-frame B. However, we

Table 1. APM astrometry, and 2MASS NIR and SCUBA submm photometry of $z \sim 2$ quasars.

Target name	RA (J2000)	Dec. (J2000)	z	J	H	M_B^{Λ} ($M_B^{\rm EdS}$)	Observation Dates	$S_{850} \pm \sigma_{850}$ (mJy)	Notes
(1)	(2)	(3)	(4)	(5)	(6)	(7)	(8)	(9)	(10)
LBQS B0018−0220[a]	00 21 27.37	−02 03 33.8	2.56	16.2	15.4	−28.6(−28.3)	05/08/00	17.2±2.9	
HS B0035+4405[a]	00 37 52.31	+44 21 32.9	2.71	15.9	15.4	−28.7(−28.4)	22/09/00	9.4±2.8	
HS B0211+1858	02 14 29.71	+19 12 37.6	2.47	16.2	15.5	−28.3(−28.0)	22/09/00	7.1±2.1	
HS B0810+2554[b]	08 13 31.30	+25 45 02.9	1.50	14.1	13.2	−29.2(−29.1)	07,09,10/08/00	7.6±1.8	
HS B0943+3155	09 46 23.21	+31 41 30.5	2.79	16.5	16.0	−28.1(−27.8)	08/10/00	9.6±3.0	
HS B1140+2711	11 42 54.27	+26 54 57.8	2.63	15.8	15.2	−28.8(−28.5)	17/01/01	8.6±2.6	
HS B1141+4201	11 43 52.04	+41 45 19.8	2.12	15.5	15.1	−28.5(−28.3)	18/01/01	8.6±2.6	BAL
HS B1310+4308	13 12 48.73	+42 52 36.8	2.60	16.0	15.8	−28.2(−27.9)	13/04/01	10.0±2.8	weak BAL
HS B1337+2123	13 40 10.84	+21 08 44.5*	2.70	16.5	15.6	−28.4(−28.1)	13/04/01	6.8±2.1	
LBQS B0009+0219	00 12 19.64	+02 36 35.4	2.64	16.3	16.0	−28.0(−27.7)	06/08/00	1.4±3.2	
LBQS B0009−0138	00 12 10.91	−01 22 07.7	2.00	16.2	15.7	−27.6(−27.4)	06/08/00	2.2±2.8	
LBQS B0013−0029	00 16 02.41	−00 12 25.2	2.08	16.3	15.2	−27.7(−27.5)	06/08/00	3.2±3.3	
HS B0017+2116	00 20 10.85*	+21 32 51.4*	2.02	16.0	15.5	−27.8(−27.6)	22/09/00	2.3±3.0	
LBQS B0025−0151	00 27 33.82	−01 34 52.4	2.08	16.3	15.7	−27.7(−27.5)	06/08/00	4.8±2.4	BAL
HS B0029+3725[c]	00 32 10.08	+37 42 32.5	1.85	15.8	15.5	−28.6(−28.4)	14/09/00	2.2±2.6	
HS B0036+3842	00 39 07.49	+38 59 15.5*	2.36	16.4	15.6	−28.0(−27.7)	22/09/00	3.0±3.0	BAL
HS B0037+1351	00 40 23.76	+14 08 07.5	1.87	15.6	15.1	−28.1(−27.9)	06/08/00	3.4±3.1	
HS B0042+3704	00 44 48.3†	+37 21 14†	2.41	16.4	15.9	−28.0(−27.7)	12/10/00	−1.2±2.6	
HS B0105+1619	01 08 06.47	+16 35 50.4	2.64	15.7	15.1	−28.9(−28.6)	04/08/00	3.8±2.6	
HS B0119+1432	01 21 56.06	+14 48 24.0	2.87	15.5	15.1	−29.0(−28.7)	04/08/00	3.6±2.6	
HS B0150+3806	01 53 13.55	+38 21 24.2	1.96	16.0	15.4	−27.8(−27.6)	06/08/00	2.2±3.0	
HS B0202+1848	02 05 27.52	+19 02 29.8	2.70	15.7	15.3	−28.8(−28.5)	05/08/00	0.6±3.3	
HS B0218+3707	02 21 05.52	+37 20 46.2	2.41	15.8	14.9	−28.6(−28.4)	04/08/00	1.9±2.6	
HS B0219+1452	02 22 31.71*	+15 06 28.6*	1.71	14.8	14.2	−28.8(−28.6)	05/08/00	−5.3±2.8	
HS B0248+3402	02 51 27.78	+34 14 42.1	2.23	15.4	15.0	−28.6(−28.4)	04/08/00	−0.2±2.7	
HS B0752+3429	07 55 24.10	+34 21 34.2	2.11	16.1	15.4	−27.9(−27.7)	22/09/00	2.4±2.8	
HS B0800+3031	08 03 42.05	+30 22 54.8	2.02	15.1	14.5	−28.8(−28.6)	07/07/00	−3.0±3.4	
HS B0808+1218	08 10 56.9†	+12 09 14†	2.26	16.2	15.5	−28.0(−27.8)	22/09,08/10/00	1.1±2.1	
HS B0821+3613	08 25 07.66	+36 04 11.5	1.58	15.5	14.7	−27.9(−27.7)	22/09,08/10/00	1.5±2.0	
HS B0830+1833	08 32 55.63	+18 23 00.7	2.27	15.9	15.4	−28.3(−28.1)	08/10/00	−0.5±3.1	
HS B0834+1509	08 37 12.87*	+14 59 17.5	2.51	16.2	15.4	−28.3(−28.0)	08/10/00	−1.0±2.8	
HS B0926+3608	09 29 52.14	+35 54 49.8	2.14	16.3	15.5	−27.7(−27.5)	08/10/00	1.2±2.8	
HS B0929+3156	09 32 08.77	+31 43 28.0*	2.08	16.1	15.6	−27.9(−27.7)	08/10/00	5.7±3.0	weak BAL
HS B0931+2258	09 34 42.26	+22 44 39.5	1.74	15.4	14.8	−28.2(−28.0)	08/10/00	−3.5±2.8	
HS B1002+4400	10 05 17.47	+43 46 09.3	2.08	15.5	15.0	−28.5(−28.3)	13,19/04/01	8.2±2.9	
HS B1031+1831	10 34 28.89	+18 15 32.4	1.53	15.1	14.3	−28.3(−28.1)	19/04/01	−0.1±2.7	BAL
HS B1049+4033	10 51 58.71*	+40 17 37.0*	2.15	15.7	15.1	−28.4(−28.2)	19/04/01	3.9±3.2	
HS B1111+4033	11 13 50.94*	+40 17 21.5	2.18	16.0	15.7	−28.1(−27.9)	19/04/01	2.2±2.8	
HS B1115+2015	11 18 00.52*	+19 58 53.8*	1.93	15.5	15.0	−28.4(−28.2)	19/04/01	5.3±2.8	BAL
HS B1126+3639	11 28 57.84*	+36 22 50.3*	2.89	16.3	15.8	−28.3(−28.0)	19/04/01	−2.5±2.8	
HS B1155+2640	11 57 41.91	+26 23 56.2	2.80	16.6	15.8	−28.3(−28.0)	19/04/01	3.5±2.7	
HS B1200+1539	12 03 31.28*	+15 22 54.4*	2.97	15.8	15.2	−28.9(−28.6)	08/01/01	−5.1±3.1	
LBQS B1210+1731[d]	12 13 03.02	+17 14 23.4*	2.54	16.3	15.6	−28.3(−28.0)	08/01/01	1.3±2.8	
HS B1215+2430	12 18 10.98	+24 14 10.8	2.36	15.8	15.1	−28.6(−28.3)	19/04/01	6.0±2.7	
HS B1302+4226	13 04 25.56	+42 10 09.7	1.91	15.3	14.7	−28.5(−28.3)	18/01/01	2.4±2.4	weak BAL
HS B1326+3923	13 28 23.73*	+39 08 17.8	2.32	15.4	14.8	−28.8(−28.6)	08/01/01	7.4±3.0	
LBQS B1334−0033	13 36 47.16	−00 48 57.4	2.80	16.3	15.6	−28.0(−27.8)	08/01/01	2.5±2.6	
HS B1356+3113	13 59 08.39	+30 58 30.8	2.26	16.2	15.7	−28.6(−28.3)	20/03/01	3.2±3.0	
HS B1417+4722	14 19 51.84	+47 09 01.1	2.27	15.7	15.1	−28.5(−28.3)	18/01/01	8.8±3.4	
HS B1422+4224	14 24 35.96	+42 10 30.6*	2.21	16.2	16.0	−27.7(−27.5)	19/04/01	10.7±4.7	
HS B1703+5350	17 04 06.74	+53 46 53.6	2.37	15.9	15.3	−28.4(−28.1)	20/03/01	−0.1±2.6	
HS B1754+3818	17 56 39.6†	+38 17 52†	2.16	16.0	15.4	−28.1(−27.9)	20/03/01	0.7±2.5	
HS B2134+1531	21 36 23.86*	+15 45 08.4	2.13	15.6	14.8	−28.4(−28.2)	04/08/00	−0.2±2.9	
LBQS B2244−0105	22 46 49.30	−00 49 53.9	2.03	15.9	15.7	−27.9(−27.7)	14/09/00	0.2±2.8	
HS B2245+2531	22 47 27.40	+25 47 30.5	2.15	15.4	14.9	−28.5(−28.3)	04/08/00	3.5±2.6	
HS B2251+2941	22 53 38.59	+29 57 12.5	1.57	15.5	14.7	−27.9(−27.7)	14/09/00	−1.2±2.6	
HS B2337+1845	23 39 44.77*	+19 01 51.1	2.62	15.6	14.9	−29.1(−28.8)	04/08/00	2.4±4.0	

a. Detected at 450μm (Isaak et al., in prep.); b. *IRAS* source, $S_{60} = 284 \pm 40$mJy, $S_{100} = 538 \pm 160$mJy. Recent *HST* STIS imaging shows this quasar to be quadrupally lensed (Reimers et al. 2002); c. $S_{1.4\rm GHz} = 2.6$mJy; d. $S_{1.4\rm GHz} = 2.0$mJy

* APM position offset from published coordinates by 1 arcsec or more: 2MASS position favours APM

† blending in APM, published (HS) coordinates used

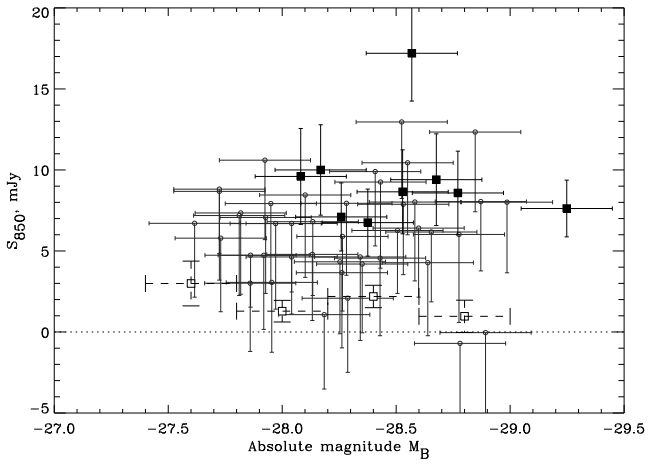

Figure 3. 850μm flux against absolute B magnitude (Λ cosmology) for the complete $z \approx 2$ SCUBA sample. Submm detections are plotted as large solid squares with error bars reflecting photometric errors in S_{850} and NIR magnitudes. Non-detections are plotted in light grey, as upper limits corresponding to signal + 90% confidence, with a vertical error bar terminating at the value of the signal. The weighted means of the non-detections in each of four magnitude bins are also plotted as open symbols.

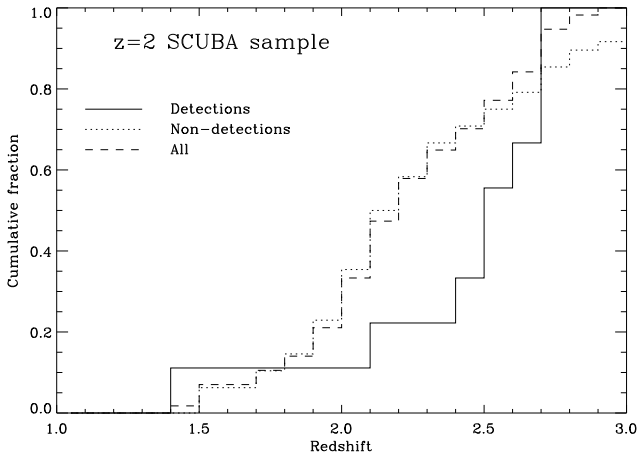

Figure 4. Cumulative histogram for redshifts of the $z \approx 2$ SCUBA sample. The difference between the distributions of the detected (solid) and undetected (dotted) and parent (dashed) samples is clear to the eye, and supported by formal statistics.

can use them to assess, roughly, whether there is any correlation between submm detectability and optical colour— for example, whether submm excess is connected with intrinsic reddening. The mean $B-H$ colour of the sample is 1.9±0.5, whereas that of the detections is 2.0±0.5; similarly, $B-J$ of the sample is 1.3±0.4, of the detections 1.4±0.5. There is no evidence, then, that the detected quasars are redder than the underlying sample. However, given the large uncertainties, further work is required to address the question systematically.

Note that while we are requiring our sample to be bright in rest-frame B, the selection procedure for these surveys (e.g. LBQS $B_J < 18.75$) also requires these objects to be bright in the rest-frame UV. This limit in observed B translates into a limit on redness for a given luminosity at a given redshift. In the very worst case ($z = 3$, $M_B = -27.5$), objects redder than $\alpha = -0.7$ are excluded. On the other hand, by selecting objects bright in 2MASS, we are biased against very blue quasars. There is, however, no statistically significant correlation between colour and either M_B or z; and the distribution of spectral indices for the sample is similar to (if a little narrower than) that of the whole LBQS (median $\alpha = -0.3$, Francis et al. 1991).

4.3 Broad Absorption Line Quasars

Omont et al. (1996) suggested that those quasars exhibiting broad absorption lines (BALs) in their optical spectra are preferentially detected in the submm. This is based on the marginal evidence that two out of their six $z > 4$ IRAM detections were BALs, relative to the background BAL abundance of $\approx 10\%$ (Weymann et al., 1991). We are now in a better position to test this hypothesis. Considering sources from the current paper, one of the detections (HS B1141+4201) is unambiguously a BAL, another (HS B1310+4308) is possibly a weak BAL. In comparison, four of the non-detections are BALs, with a number of others showing signs of weak absorption, a fraction consistent with the expected 10%. Thus, although far from providing proof, these data do not rule out the Omont et al. hypothesis. In a forthcoming paper (Priddey et al., in prep.), we shall discuss, in detail, the evidence from a statistically-significant combination of all recent submm and mm quasar surveys.

4.4 Submillimetre versus redshift

Figure 4 is a cumulative histogram of redshift for the $z \sim 2$ sample and for the detected subsample. The distributions appear different to the eye, with most of the detections lying at higher redshift. The median redshift of the sample is $z = 2.3$ and that of the detections $z = 2.6$. The maximum difference between the distributions of detected and parent samples is 0.42, corresponding to a K–S level of significance 5 percent,whilst for the the detected and undetected samples, the maximum is 0.51, giving a level of significance ≈1 percent. Within this limited redshift range, therefore, there is a suggestion that the submm detection rate increases with redshift over the range $1.5 < z < 3.0$. In Figure 5, the far-infrared luminosity as a function of redshift has been derived by calculating the σ^{-2}-weighted mean of *all* the SBQS data— I02 for $z > 3$, and the current work for $z < 3$— and for detections and non-detections alike. 850μm flux has been converted to a luminosity assuming the isothermal SED derived in PM01. Changing this assumption would shift the $z > 4$ and $z \sim 2$ points relative to one another (*lowering* the temperature or β *increases* the relative luminosity of the $z > 4$ points). In I02, the fluxes of the non-detections were stacked to give an estimate of the submm flux of an average $z > 4$ quasar— after checking that sky-subtraction had been performed effectively, by observing that the distribution of the signal in all off-source pixels is a Gaussian with zero mean. We repeat the experiment with the current $z \sim 2$ data, and obtain $S = 1.9 \pm 0.4$mJy, which agrees within the uncertainties with the $z > 4$ value, 2.0 ± 0.6mJy.

We can compare these results with those drawn from the SCUBA survey of high-redshift radio galaxies (Archibald et al., 2001), from which a dramatic increase of FIR luminosity with redshift was inferred, $L_{\rm FIR} \sim (1+z)^{3-4}$, over the whole redshift range $1 < z < 4$ (see Figure 5). While our tentative low-redshift decline echoes this behaviour, the difference between $z > 4$ and $z = 2$ is far less marked. It is necessary to improve the statistics and to consider the selection effects before drawing firm conclusions. Nevertheless, the disparity between the two populations is a potentially revealing commentary on the nature of radio loudness in AGN. Conceivably, radio galaxies follow a more dramatic evolution than the majority of AGN— of which they are perhaps the most extreme members— their radio-loudness originating from a difference in formation mechanism. Note however that the masses of their central black holes may be no more extreme than those of the most optically-luminous radio-*quiet* quasars in the present sample, some of which would have $M > 10^9\,{\rm M}_\odot$, even assuming accretion at the maximum (Eddington) rate.

The present results show that, on average, the submm properties of luminous, radio-quiet quasars at $z \sim 2$ are comparable, within the uncertainties, to those at $z > 4$, despite the lack of brighter sources in the present sample. Although the uncertainties are too great to draw detailed conclusions, one can speculate on the physical processes underlying the redshift variation of submm detectability at fixed optical luminosity. In a starburst scenario, for example, the gas accretion efficiency and the star formation efficiency could each depend in a different way upon redshift (*e.g.* through the dynamical time: Kauffmann & Haehnelt, 2000). At $z > 4$, the host galaxy is presumably gas- (and dust-) rich, whereas by $z < 2$ most of the gas has formed into stars. At yet higher redshifts ($z > 5$) the youth of the universe may preclude the production of enough obscuring dust for the quasar to be a luminous submm source (Priddey et al., in prep.). Expanding the redshift range of Figure 5 in each direction is a project currently in progress, but at present it is intriguing that the average submillimetre loudness seems to decline when the population itself declines.

4.5 Caveat: gravitational lensing

A factor that we have *not* addressed in deriving this result is the influence of gravitational lensing. In common with many of bright submillimetre sources found in surveys, it is likely that fluxes are boosted by lensing. This is likely to lead to bias, as the lensing optical depth increases with redshift (e.g. Barkana & Loeb, 2000). Thus the $z > 4$ sources are likely to be intrinsically fainter than they appear, relative to those at $z = 2$. Considering individual sources, *HST* STIS imaging (after the current data were obtained) showed HS0810+2554 to be lensed into a quadruple source with a tight (<1 arcsec) separation between the components (Reimers et al. 2001). This explains the extremely high infrared luminosity implied by its detection in the *IRAS* Faint Source Catalogue.

We stress that *no corrections* for lensing have been applied in the current work, for this is complex and model-dependent. However, this important issue will be tackled in quantitative detail in a future paper (Priddey et al., in prep.), where we present a detailed statistical analysis of all recent JCMT/SCUBA and IRAM/MAMBO high-redshift quasar data.

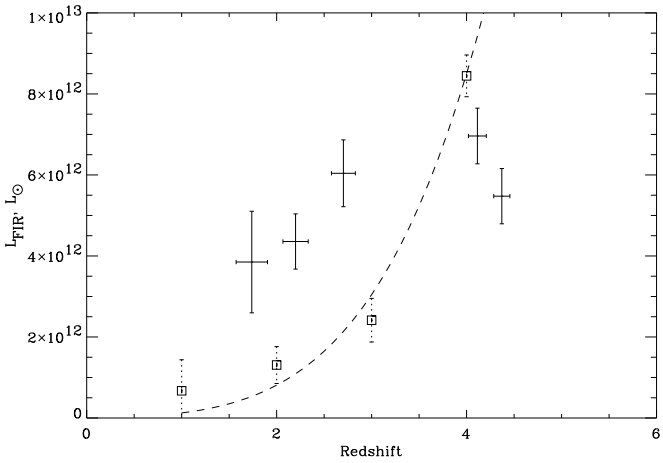

Figure 5. FIR luminosity for SBQS quasars (crosses) as a function of redshift, determined from the weighted mean of all data within each bin. Also plotted, for comparison, are the radio galaxy points (squares) and the power-law fit from Archibald et al. (2001).

5 SUMMARY AND FUTURE WORK

In this paper, we have presented the first results from a targetted SCUBA survey of optically-luminous ($M_B < -27.5$), radio-quiet quasars at $z \sim 2$. This is a continuation of the SCUBA Bright Quasar Survey whose preliminary results, at $z > 4$, were reported by Isaak et al. (2002). The present data confirm the presence of a large scatter in the correlation between submm and optical luminosity, despite having minimized the errors in measurement of the latter. Comparing the $z > 4$ and $z < 3$ datasets shows that there is no evidence for a variation of submm properties of luminous quasars across this redshift range, once one has allowed for a K-correction appropriate for cool, isothermal dust. However, there is a suggestion that the characteristic submm luminosity increases with redshift between $z = 1.5$ and $z = 3$. We note that a companion survey, carried out at 1.2mm with the MAMBO array on the IRAM 30m telescope, reaches similar conclusions (Omont et al. 2002).

In forthcoming papers, we shall present multiwavelength follow-up of bright sources from the present sample, results of comparative studies to improve the redshift coverage, detailed statistical analysis of >200 high-redshift quasars observed at (sub)mm wavelengths, and astrophysical interpretation of the findings.

ACKNOWLEDGMENTS

For support through the period during which the bulk of this work was carried out, RSP and KGI thank PPARC and RGM thanks the Royal Society. We are grateful to the JACH staff and those JCMT observers, their projects displaced by poor weather, who gathered data for us in fallback mode. The JCMT is operated by JAC, Hilo, on behalf of the

parent organisations of the Particle Physics and Astronomy Research Council in the UK, the National Research Council in Canada and the Scientific Research Organisation of the Netherlands. We thank the anonymous referee for constructive comments.

REFERENCES

Archibald E.N., Dunlop J.S., Hughes D.H., Rawlings S., Eales S.A., Ivison R.J., 2001, MNRAS, 323, 417
Barkana R. & Loeb A., 2000, ApJ, 531, 613
Cutri R.M. et al., 2000, *Explanatory Supplement to the 2MASS Second Incremental Data Release*, http://www.ipac.caltech.edu/2mass/releases/second/doc/explsup.html
Engels D., Hagen H.-J., Cordis L., Koehler S., Wisotzki L., Reimers D., 1998, AAPS, 128, 507
Fan X. et al., 2001, AJ, 121, 54
Francis P.J., Hewett P.C., Foltz C.B., Chaffee F.H., Weymann R.J., Morris S.L., 1991, ApJ, 373, 465
Hagen H.-J., Engels D., Reimers D., 1999, AAPS, 134, 483
Hewett P.C., Foltz C.B. & Chaffee F.H., 1995, AJ, 109, 1498
Hughes D.H., Robson E.I., Dunlop J.S., Gear W.K., 1993, MNRAS, 263, 607
Isaak K.G., Priddey R.S., McMahon R.G., Omont A., Cox P., Peroux C., Sharp R., Withington S., 2002, MNRAS, 329, 149 (I02)
Kauffmann G. & Haehnelt M., 2000, MNRAS, 311, 576
Madau P. et al., 1996, MNRAS, 283, 1388
Magorrian J. et al., 1998, AJ, 115, 2285
McMahon R.G., Priddey R.S., Omont A., Snellen I., Withington S., 1999, MNRAS 309, L1 (M99)
Omont A., McMahon R.G., Cox P., Kreysa E., Bergeron J., Pajot F., Storrie-Lombardi L.J., 1996a, A&A, 315, 1
Omont A., Cox P., Bertoldi F., McMahon R.G., Carilli, C., Isaak K.G., 2001, A&A, 374, 371
Omont A., Beelen A., Bertoldi F., Cox P., Carilli, C., Priddey R.S., McMahon R.G., Isaak K.G., 2002, accepted by A&A
Priddey R.S. & McMahon R.G., 2001, MNRAS, 324, L17 (PM01)
Reimers D., Hagen H.-J., Baade R., Lopez S., Tytler D., 2002, A&A, 382, L26
Rowan-Robinson M., 2000, MNRAS, 316, 885
Schmidt M., Schneider D.P., Gunn J.E., 1995, AJ, 110, 68
Steidel C., et al., 1999, ApJ, 519, 1
Weymann R.J., Morris S.L., Foltz C.B., Hewett P.C., 1991, ApJ, 373, 23